

Accepted Manuscript

Column studies to assess the effects of climate variables on redox processes during riverbank filtration

Matthias Rudolf von Rohr , Janet G. Hering , Hans-Peter E. Kohler , Urs von Gunten



PII: S0043-1354(14)00371-6

DOI: [10.1016/j.watres.2014.05.018](https://doi.org/10.1016/j.watres.2014.05.018)

Reference: WR 10672

To appear in: *Water Research*

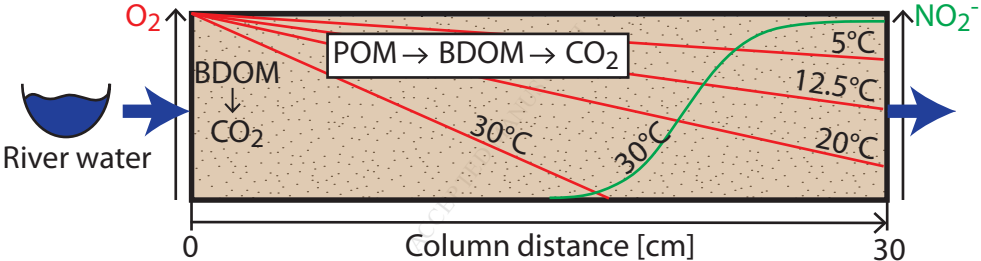
Received Date: 25 February 2014

Revised Date: 10 May 2014

Accepted Date: 12 May 2014

Please cite this article as: Rudolf von Rohr, M., Hering, J.G., Kohler, H.-P.E., von Gunten, U., Column studies to assess the effects of climate variables on redox processes during riverbank filtration, *Water Research* (2014), doi: 10.1016/j.watres.2014.05.018.

This is a PDF file of an unedited manuscript that has been accepted for publication. As a service to our customers we are providing this early version of the manuscript. The manuscript will undergo copyediting, typesetting, and review of the resulting proof before it is published in its final form. Please note that during the production process errors may be discovered which could affect the content, and all legal disclaimers that apply to the journal pertain.



**Column studies to assess the effects of climate variables on redox
processes during riverbank filtration**

Matthias Rudolf von Rohr^{1,2}, Janet G. Hering^{1,2,3}, Hans-Peter E. Kohler^{1,2}, Urs von
Gunten^{1,2,3,*}

¹ EAWAG, Swiss Federal Institute of Aquatic Science and Technology, Water

Resources & Drinking Water, Überlandstrasse 133, 8600 Dübendorf, Switzerland

² ETH Zürich, Institute of Biogeochemistry and Pollutant Dynamics, Universitätstrasse
16, 8092 Zürich, Switzerland

³ Ecole Polytechnique Fédérale de Lausanne (EPFL), School of Architecture, Civil and
Environmental Engineering (ENAC), 1015 Lausanne, Switzerland

*Corresponding author

Urs von Gunten

Überlandstrasse 133

P.O. Box 611

Phone: +41 58 765 5270

Fax: +41 58 765 5210

urs.vongunten@eawag.ch

Highlights

- Effects of climate variables on redox processes were tested in column studies
- Biodegradable dissolved organic matter was removed immediately at the column inlet
- Oxygen consumption was attributed to respiration of particulate organic matter
- Temperature and infiltration rate strongly affected the oxygen consumption
- Nitrate acted as a redox buffer preventing Mn(II) mobilization

Abstract

Riverbank filtration is an established technique used world-wide to produce clean drinking water in a reliable and cost-efficient way. This practice is, however, facing new challenges posed by climate change, as already observed during past heat waves with the local occurrence of anoxic conditions. In this study we investigated the effect of direct (temperature) and indirect (dissolved organic matter (DOM) concentration and composition, flow rate) climate change variables on redox processes (aerobic respiration, denitrification and Mn(III/IV)/Fe(III) reduction) by means of column experiments. Natural river water, modified river water and river water mixed with treated wastewater effluent were used as feed waters for the columns filled with natural sand from a river-infiltration system in Switzerland. Biodegradable dissolved organic matter was mainly removed immediately at the column inlet and particulate organic matter (POM) associated with the natural sand was the main electron donor for aerobic respiration throughout the column. Low infiltration rates (≤ 0.01 m/h) enhanced the oxygen consumption leading to anoxic conditions. DOM consumption did not seem to be sensitive to temperature, although oxygen consumption (i.e., associated with

POM degradation) showed a strong temperature dependence with an activation energy of $\sim 70 \text{ kJmol}^{-1}$. Anoxic conditions developed at 30°C with partial denitrification and formation of nitrite and ammonium. In absence of oxygen and nitrate, Mn(II) was mobilized at 20°C , highlighting the importance of nitrate acting as a redox buffer under anoxic conditions preventing the reductive dissolution of Mn(III/IV)(hydr)oxides. Reductive dissolution of Fe(III)(hydr)oxides was not observed under these conditions.

Keywords: climate change; redox milieu; microbial respiration; effluent ; POM; BDOM

1 Introduction

Several European countries rely on natural or engineered riverbank filtration to produce drinking water, with a contribution of $< \sim 50\%$ to the total drinking water production in France (Hannappel et al., 2014), $\sim 16\%$ in Germany (Tufenkji et al., 2002) and $\sim 25\%$ in Switzerland. During riverbank filtration, river water infiltrates through riverbed sediments into an aquifer, from which it is extracted for drinking water production. The derived groundwater often requires only minimal treatment before distribution, because natural attenuation processes during infiltration efficiently remove particles, microorganisms, natural organic matter (NOM) and partially remove organic contaminants (Kuehn and Mueller, 2000; Grünheid et al., 2005; Schmidt et al., 2007; Scheurer et al., 2012; Storck et al., 2012; Huntscha et al., 2013).

An important criteria for the quality of drinking water derived from riverbank filtration is the redox milieu and the related geochemical processes. The redox milieu is mainly determined by microbial respiration processes (redox processes), in which NOM is the electron donor and oxygen, nitrate, Mn(III/IV)- and Fe(III)(hydr)oxides or

sulfate are the electron acceptors. These biogeochemical processes have been extensively studied at riverbank filtration sites (Jacobs et al., 1988; Bourg and Bertin, 1993) and in laboratory column experiments (Matsunaga et al., 1993; von Gunten and Zobrist, 1993). Seasonal changes in the redox milieu, in which anoxic (i.e. oxygen-free) conditions develop and Mn(II) is mobilized in summer and aerobic conditions are maintained in winter, have been ascribed to the temperature dependence of microbial activity (von Gunten et al., 1991; Greskowiak et al., 2006; Massmann et al., 2006).

Besides temperature, the quantity and composition of NOM in river waters also dictate the redox milieu during riverbank filtration, since NOM is an important substrate for microbial respiration (Grünheid et al., 2005; Maeng et al., 2008). Previous studies have focused on dissolved organic matter (DOM) as the main electron donor during riverbank filtration (von Gunten and Zobrist, 1993; Grünheid et al., 2005; Grünheid et al., 2008; Maeng et al., 2008). However, there is evidence that particulate organic matter (POM) in the riverbed sediments may also contribute substantially as a substrate to the consumption of electron acceptors (Grischek et al., 1998; Brugger et al., 2001; Massmann et al., 2006; Diem et al., 2013b).

Furthermore, the hydraulic residence time, which is determined by the infiltration rate, may influence the redox milieu during riverbank filtration. It is assumed that low infiltration rates favor and high infiltration rates inhibit the formation of reducing conditions in the aquifer (Doussan et al., 1997). Drought periods generally tend to bring about anaerobic conditions during summer months as a consequence of long residence times and high temperatures, whereas floods tend to increase the infiltration rate and facilitate the breakthrough of pathogens, suspended solids and DOM (Sprenger et al., 2011). Moreover, flood events can also lead to an increased oxygen consumption in the infiltration zone, which has been attributed to an increased deposition of POM in this zone under these conditions (Diem et al., 2013b).

All factors that dictate the redox milieu in the riverbank filtration zone may be directly (temperature) or indirectly (NOM quantity and composition in river water, residence time in the infiltration zone) influenced by climate and climate change. By 2085, average summer air temperatures in northern Switzerland are predicted to increase by 4 K and average summer precipitation to decrease by 20% resulting in lower discharges in rivers (CH2011, 2011; FOEN, 2012). The lower river discharges may also lead to lower infiltration rates and thus longer hydraulic residence times in the infiltration zone. In addition, decreasing natural flows will reduce the extent to which effluent organic matter (EfOM) discharged from wastewater treatment plants is diluted and consequently a higher proportion of EfOM in the receiving waters may be expected. Better understanding of the effect of each climate factor on the redox milieu will help to assess future changes in water quality during riverbank filtration.

We hypothesize that the direct and indirect effects of climate change will lead to more frequent occurrence of anoxic conditions in riverbank filtration systems in the future. This could create significant problems for drinking water supplies because of the potentially more frequent occurrence of reduced species, such as nitrite, Mn(II) and Fe(II). Nitrite is a toxic compound for which the WHO guideline is 900 µg N/L (WHO, 2011). When groundwater containing Mn(II) and Fe(II) is exposed to oxygen from the air, the resulting precipitation of Mn(III/IV)- or Fe(III)(hydr)oxides can cause clogging of filter screens and lead to rusty water and aesthetic problems (Mouchet, 1992; Hoehn and Scholtis, 2011).

Here, we assess the effect of direct and indirect climate change variables on redox conditions during riverbank filtration based on column experiments, in which temperature, DOM concentration/composition and flow rate were systematically varied. Moreover, the dynamics of the Mn(II) and Fe(II) mobilization under oxygen- and nitrate-free conditions were investigated.

2 Materials and Methods

2.1 Set-up of the column system

Fig. S1 shows the set-up of the column system: Filtered Thur River water (0.45 μm , cellulose nitrate, Sartorius AG, Göttingen, Germany) was pumped from the bottom to the top of the column with a HPLC-pump (Jasco PU-2080, Jasco Corporation, Tokyo, Japan). The casing of the column consisted of a Plexiglas tube (length: 30 cm, inner diameter: 5.2 cm). The column was equipped with 13 sampling ports (SP1-13), in addition one was installed before (SP0) and one after (SP14) the column (Fig. S1). The column was packed with a dried sand fraction (grain size: 0.125-0.250 mm) sampled at a sand/gravel bar at the Thur River (Diem et al., 2013b). The relatively homogeneous sand fraction 0.125-0.250 mm contained $0.3 \pm 0.2\%$ (w/w, average of 12 sample aliquots) particulate organic carbon (POC). The filling procedure of the dry sand was conducted in form of a “sand rain”, following von Gunten and Zobrist (1993). X-ray diffraction analysis of the sand showed mainly calcite and quartz (40% and 25%, respectively). Two columns (column I and II) filled with the same sand material were used for the respective experiments under different operational conditions (Section 2.2). We assessed the hydraulics in columns I and II by conducting tracer tests with a 8.55 mM NaCl solution. During the tracer tests, the electrical conductivity was measured at the end of the columns and was used for the calculation of the effective porosity and the dispersivity (Table 1).

River water was collected at Niederneunforn at a river-infiltration system of the peri-alpine Thur River, NE-Switzerland (Diem et al., 2013b), filtered and used as feed water from a 2 L storage tank (see Table S1 for chemical composition of all feed waters). The storage tank was replenished every three days with Thur River water stored at 5°C. For the experiments performed at 12.5°C, 20°C and 30°C, Thur River

water was equilibrated to the desired temperature before it was pumped into the columns. No measurable DOM degradation (DOC concentration ± 0.1 mg C/L) was observed in the storage tank under these conditions.

For varying operational conditions, the profiles of the oxygen concentration were taken for steady-state conditions after an equilibration time of ≥ 20 d. Sampling was conducted from the top to the bottom of the column in the opposite direction of the water flow (Fig. S1). This procedure enabled sampling of fresh aliquots avoiding sampling from stagnant zones. Oxygen and pH were directly measured at each sampling port in a flow-through cell having a total dead volume of ~ 3 mL (Fig. S1). For the analysis of DOC, major cations and anions, a $0.45 \mu\text{m}$ rinsed regenerated cellulose filter (National Scientific Company, Rockwood, USA) was connected to the port of interest and a ~ 40 mL sample was withdrawn for each sampling event (duration of sampling: ~ 40 minutes at 1 mL/min). Oxygen, pH, DOC and nitrate were measured between one and three times every 3-5 days (indicated in the figures by “n”, i.e. the number of measurement replicates). For Fe and Mn analysis, a 9 mL sample was acidified to pH 2 with 1 mL of 1 M HCl.

(Table 1)

2.2 Operational conditions of the column experiments

Six different column experiments with varying parameters (feed water, temperature, flow rate) were conducted either with column I or II (Table 2). The first experiments for each column (experiment 1.1 for column I and experiment 2.1 for column II, respectively) were initiated after an equilibration time of 2 months feeding Thur River water to reach steady-state conditions for oxygen and DOC.

For experiment 1.1, treated wastewater effluent (herein simply named effluent) from a municipal wastewater treatment plant (Dübendorf Neugut, Switzerland) was first filtered (0.45 μm , cellulose nitrate, Sartorius AG, Göttingen, Germany). The filtered effluent was then electrodialysed (PCCell GmbH, Heusweiler, Germany) to remove nitrate prior to preparing four Thur River water/effluent mixtures to be used as feed waters (Tables S1 and S2) to study the effect of the type and concentration of DOM on the oxygen consumption.

In experiment 1.2, the effect of the flow rate on the oxygen consumption was investigated. Four flow rates, simulating different infiltration velocities, were chosen: 0.1, 0.2, 0.33 and 1.0 mL/min.

In experiment 2.1, the temperature dependence of the oxygen consumption and NOM degradation was investigated at four temperatures (5, 12.5, 20 and 30°C). While the experiments at 5.0, 12.5 and 20.0°C were carried out with the storage tank at ambient laboratory temperature ($22 \pm 2^\circ\text{C}$), for the 30.0°C experiment the tank had to be placed inside the incubator to prevent outgassing in the HPLC-pump.

In experiment 2.2, unaltered Thur River water was added as feed water and in experiment 2.3, "DOM-free" Thur River water was used as feed water to study the effect of POM on the oxygen consumption. About 96% of the DOM was removed from the Thur River water by addition of 500 mg/L Norit W15 powdered activated carbon (NORIT Deutschland GmbH, Riesbürg, Germany) and filtration through a 0.45 μm filter (cellulose nitrate, Sartorius AG, Göttingen, Germany). DOM removal was achieved without significantly affecting the other water quality parameters (Table S3).

In experiment 2.4, a readily available DOM source in form of sodium acetate (6 mg/L or 1.75 mg C/L) was added to the Thur River water inflow immediately before the column inlet (at sampling port SP0) to investigate the effect of easily biodegradable DOM (BDOM) on the oxygen consumption.

In experiment 2.5, the dynamics of the Mn(II) and Fe(II) mobilization under oxygen- and nitrate-free conditions were investigated. Thur River water was electro dialysed to remove nitrate and was re-mineralized thereafter to obtain a similar water composition as the original river water with respect to the alkalinity and the major cations and anions (Table S4). To remove oxygen from the feed water, it was continuously purged with a N₂/CO₂ gas mixture (99.96% N₂ / 0.04% CO₂) leading to an oxygen concentration below 0.1 mg/L at SP0.

All column experiments except 1.1 and 1.2 were conducted in an incubator ($\pm 1^\circ\text{C}$). Column experiment 1.1 was carried out at ambient laboratory temperature ($22 \pm 2^\circ\text{C}$) and experiment 1.2 in a climatised chamber ($20 \pm 1^\circ\text{C}$). Column I was operated aerobically (experiments 1.1 and 1.2), whereas column II was first operated aerobically for 327 days (experiments 2.1, 2.2, 2.3 and 2.4) and then anaerobically for 66 days (experiment 2.5).

(Table 2)

2.3 Analytical methods

Oxygen and temperature were measured with an optical sensor LDO101 (Hach Lange GmbH, Berlin, Germany, limit of quantification 0.1 mg/L, accuracy ± 0.1 mg/L, $T \pm 0.3$ K), pH was measured with a pH electrode PHC 301 (Hach Lange GmbH, Berlin, Germany, accuracy pH ± 0.1). DOC was taken as a measure for DOM and was determined by catalytic combustion at 720°C with a Shimadzu TOC-V CPH analyzer (Shimadzu Corporation, Kyoto, Japan). The limit of quantification was 0.1 mg C/L and the error of measurement ± 0.1 mg C/L. The alkalinity was determined with a Metrohm 809 Titrando (Metrohm Schweiz AG, Zofingen, Switzerland). NO₂⁻ and NH₄⁺ were analyzed photometrically with a spectrophotometer Cary 100 Scan Spectrophotometer

(Varian AG, Zug, Switzerland) following the norms EN 26777 (DIN, 1993) and DIN 38406 (DIN, 1983a), respectively. The limit of quantification was 0.01 mg N/L and the error of measurement ± 0.002 mg N/L for both compounds. PO_4^{3-} was measured with a spectrophotometer Varian Cary 50 Bio (Varian AG, Zug, Switzerland) according to Vogler (1965). NO_3^- , Cl^- , SO_4^{2-} , Na^+ , K^+ , Ca^{2+} and Mg^{2+} were analyzed with a Metrohm 761 Compact IC (Metrohm Schweiz AG, Zofingen, Switzerland) using a "Metrohm Metrosep A Supp 5 100/4 mm" column for the anions and a "Metrohm Cation 1-2 125/4 mm" column for the cations. For NO_3^- , the limit of quantification was 0.25 mg N/L and the error of measurement ± 0.1 mg N/L. NO_3^- concentrations <0.25 mg N/L (i.e. for the preparation of the oxygen- and nitrate-free Thur River water, experiment 2.5), were measured with a spectrophotometer Varian Cary 50 Bio (Varian AG, Zug, Switzerland) according to Müller and Widemann (1955). Here, the limit of quantification was 0.1 mg N/L and the error of measurement ± 0.02 mg N/L. Fe and Mn were measured with inductively coupled plasma atomic emission spectroscopy (ICP-OES) as total Fe and total Mn concentrations, respectively (SPECTRO Analytical Instruments GmbH, Kleve, Germany). The limit of quantification was 0.1 $\mu\text{g/L}$ and the error of measurement ± 0.1 $\mu\text{g/L}$. It could be shown that total Mn corresponded to Mn(II) measured colorimetrically (DIN, 1983b).

The POC concentration of the column sand representing POM was determined by subtracting the content of inorganic carbon, measured with a CO_2 Coulometer CM5015 (UIC Inc., Joilet, USA), from the total carbon, measured with a CNS analyzer Eurovector EA3000 (Hekatech GmbH, Wegberg, Germany).

A closed bottle biological oxygen demand (BOD) test of the natural sand was conducted by BMG Engineering Ltd., Schlieren, Switzerland as a batch experiment by incubating the sand (3.2 g/L) with an inoculum of a secondary effluent from a municipal wastewater treatment plant at 22°C and measuring the decrease in the oxygen

concentration (OECD, 1992). Five batch experiments with different duration were conducted (5, 7, 14, 21 and 28 days). Each batch experiment was done in duplicate (indicated by “n=2”).

The protein content of the pristine sand and of the sand samples from column II was measured according to the bicinchoninic acid method using an assay-kit of Sigma-Aldrich (Smith et al., 1985) after protein extraction with 1 M NaOH at 95°C for 30 minutes (Herbert et al., 1971). Three samples were withdrawn from column II for each sampling port of interest (indicated by “n=3”) after 393 days of operation (i.e., at the end of experiment 2.5). The pristine sand was washed with nanopure water before protein measurements to determine the blank protein content.

The quantification of the reactive pool of Mn(III/IV)(hydr)oxides of the pristine and of the column II sand was conducted at the end of experiment 2.5 with a buffered ascorbate solution according to Hyacinthe et al. (2006). Samples were withdrawn from column II at SP1, SP5, SP8, SP11 and SP13 using a specially designed “sand scoop”. 2.6 g of each sample was mixed with a 150 mL solution consisting of sodium citrate (50 g/L), sodium bicarbonate (50 g/L) and L(+) ascorbic acid (20 g/L) (pH 7.1), which was continuously purged with N₂. The experiment was conducted for 2.5 hours and samples were taken after 0.5, 1, and 2.5 hours for ICP-OES analysis.

2.4 Calculation of manganese concentration in equilibrium with MnCO_3

The Mn^{2+} concentration in equilibrium with MnCO_3 was calculated based on the solubility product of rhodochrosite (MnCO_3) ($\text{Mn}^{2+} + \text{CO}_3^{2-} = \text{MnCO}_3$; $\log K = -10.39$ (Stumm and Morgan, 1996)) and on the CO_3^{2-} concentration of 3.34×10^{-5} M. The latter value was calculated from the measured concentration of HCO_3^- and pH (8.2) in the column during experiment 2.5. The total Mn(II) concentration was then derived by inserting the calculated Mn^{2+} equilibrium concentration, the measured calcium and HCO_3^- concentrations and the pH in the chemical equilibrium modeling program ChemEQL V3.0 (Mueller, 2004). The resulting Mn(II) speciation is shown in Table S5. The sum of all relevant Mn(II) species is shown as equilibrium concentration (Fig. S2 (dashed line)).

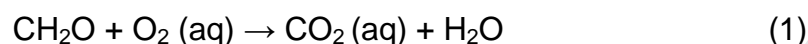
3 Results and discussion

3.1 Effect of indirect climate change variables on redox processes

3.1.1 Oxygen and pH profiles

We investigated the effects of increasing DOC concentration and altered DOM composition on redox processes by utilizing varying mixtures of Thur River water and effluent (experiment 1.1), "DOM-free" Thur River water (experiment 2.3) and Thur River water amended with acetate (experiment 2.4) as feed waters. All oxygen profiles showed a fast initial decrease of the relative oxygen concentration, which is discussed later (see Section 3.1.3), followed by a slower decrease between SP1 and SP14 (Fig. 1a). The residence times in Fig. 1a and 1b were calculated by dividing the pore volume at a specific sampling port by the flow rate of the respective experiment. The pH dropped in parallel to the fast initial oxygen drop close to the inlet and showed a slower

decrease thereafter (Fig. 1b). Both the oxygen and pH profiles can be explained by aerobic respiration (Eq. 1). The decrease of the pH, which was caused by formation of CO₂, was only partially prevented by the buffering capacity of calcium/magnesium carbonates.



In Eq. 1, CH₂O represents DOM with carbon in a zero-valent oxidation state.

(Fig. 1)

3.1.2 Role of wastewater effluent and particulate organic matter (POM)

The addition of effluent of up to 40% (experiment 1.1) did not enhance the oxygen consumption in the column (Fig. 1a) even though the DOC concentration was increased by up to 1.4 mg C/L compared with the unamended (experiment 2.2) Thur River water (see Table S1). The profile of the relative oxygen concentration of the “DOM-free” Thur River water (experiment 2.3) showed a similar decreasing trend between SP1 and SP14 as the original Thur River water (Fig. 1a). This means that the oxygen consumption did not depend on the presence of DOM in the feed water. Thur River water contains mostly humic compounds that are rather persistent (Peter et al., 2012). However, other river waters might contain significantly higher concentrations of biodegradable DOM, which could affect the oxygen consumption during riverbank filtration.

Based on our results, we hypothesize that the electron donor is associated with the sand matrix and consists of particulate organic matter (POM). Our results are in line with previous column studies conducted with river water (DOC concentration of 15

mg C/L) and a river water/effluent mixture (50% effluent, DOC concentration of 17 mg C/L) showing no enhanced oxygen consumption with the addition of a river water/effluent mixture (Maeng et al., 2008). Furthermore, it has been suggested in field investigations that POM is likely to act as an important electron donor during riverbank filtration (Griseck et al., 1998; Brugger et al., 2001; Massmann et al., 2006; Kedziorek et al., 2008; Diem et al., 2013b). These previous studies have based their conclusions on mass balance calculations of experimental field data. Here, we provide independent evidence from controlled laboratory experiments to support these field observations.

To investigate the role of POM associated with the sand as a support for aerobic respiration in the column, a biological oxygen demand (BOD) test of the pristine sand was conducted. Fig. 2 shows the BOD of the sand determined after 5, 7, 14, 21 and 28 days. Even after 28 days, the BOD had not reached a plateau; the maximum observed value was $\sim 9 \times 10^{-4}$ mg O₂/mg sand corresponding to a total BOD of at least 800 mg O₂ for the entire sand columns. If we consider that 7 mg/L oxygen was consumed on average in the column with the original Thur River water as feed water based on oxygen saturation conditions at SP0 (Fig. 1a), then ~ 3 mg O₂ will be consumed per day. The available POM could therefore sustain aerobic respiration for at least 260 days without being exhausted.

(Fig. 2)

3.1.3 Role of easily biodegradable DOM (BDOM)

The addition of acetate (1.75 mg C/L, ~ 0.14 mM C) led to an increased oxygen consumption between the first two sampling ports (Fig. 1a). The “theoretical” oxygen consumption assuming complete mineralization of the added acetate and steady-state conditions with respect to DOM sorption and desorption processes (Sobczak and

Findlay, 2002), is ~4.7 mg/L O₂ (~0.14 mM) ($\text{CH}_3\text{COOH} + 2\text{O}_2 \rightarrow 2\text{CO}_2 + 2\text{H}_2\text{O}$). This value is in good agreement with the measured oxygen consumption of 4.2 mg/L between the first two sampling ports. Therefore, this suggests that the fast initial oxygen decrease is attributed to the mineralization of acetate, as a model for BDOM, which implies that acetate and not POM was preferentially consumed at the column inlet under these conditions.

Previous results have shown that the addition of a readily available carbon source, such as lactic acid (14 mg C/L), led to a complete consumption of oxygen within the first 1.8 cm of a 30 cm column (von Gunten and Zobrist, 1993). The authors of this study also showed that the highest rate of the oxygen consumption occurred at the column inlet and was attributed to a higher microbial activity in this zone supported by a higher BDOM availability, as also demonstrated by Maeng et al. (2008).

For all experiments except for acetate addition, a similar fast initial decrease of the oxygen concentration between SP0 and SP1 could be observed (Fig. 1a). This decrease cannot be totally explained by BDOM degradation, since the differences in DOC concentrations for the Thur River water and Thur/effluent mixtures were small (<0.2 mg C/L) and below the limit of quantification for the “DOM-free” experiment. Small BDOM levels in the Thur River water could however have served as a substrate to stimulate bacterial growth leading to higher bacterial concentrations in this zone (see Section 3.2.2) allowing for a higher oxygen consumption rate associated with POM degradation.

3.1.4 Effect of flow rate

To assess the dependence of the oxygen consumption and NOM degradation on the flow rate, four experiments under different flow rate conditions (0.1, 0.2, 0.33 and 1 mL/min, i.e. residence times of 40, 20, 12 and 4 hours, respectively) were conducted

at 20°C. The profiles of the relative oxygen concentration depended on the flow rate if plotted as function of the infiltration distance (Fig. 3a), please note normalization to SP1). At the highest flow rate of 1 mL/min, oxic conditions persisted through the entire column, whereas at the flow rate of 0.2 mL/min (i.e. 0.01 m/h), anoxic conditions could be observed within 20 cm of the column inlet (Fig. 3a). Lower flow rates increased the hydraulic residence time allowing for a higher oxygen consumption in the same zone of the column and leading to anoxic conditions, which is in agreement with Doussan et al. (1997). Fig. 3b shows that the oxygen concentrations curves are superimposable when plotted against the hydraulic residence time, indicating that the differences in the residence times fully account for the observed effects of flow rate.

(Fig. 3)

3.2 Effect of direct climate change variable (temperature) on redox processes

3.2.1 Electron balance for oxygen consumption and NOM degradation

The influence of temperature on the oxygen consumption and on NOM degradation was investigated in four column experiments conducted with Thur River water at 5.0, 12.5, 20.0 and 30.0°C. The oxygen and DOM consumption (measured as difference in DOC concentration) between the column inlet and outlet is shown as a function of temperature in Fig. 4. The DOM consumption between the column inlet and outlet explained only ~30% of the oxygen consumption at 5°C and < ~7% at 12.5°C-30°C. At 30°C, the DOM consumption was lower than at the other temperatures possibly because of partial DOM degradation (~0.1 mg C/L, i.e. ~8 mM) already in the storage tank. The small contributions of the DOM consumption to the oxygen consumption for each temperature are a further confirmation for the hypothesis that POM associated

with the sand is most likely the electron donor for aerobic respiration (see Section 3.1.2).

A strong temperature dependence of the oxygen consumption could be observed between the column inlet and outlet reaching almost a plateau at 20°C (Fig. 4, white bars). Conversely, the DOM consumption between the column inlet and outlet did not seem to depend on temperature, since the values lie within the measurement uncertainty (Fig. 4, grey bars).

The small DOM consumption ($<17 \mu\text{M C}$, i.e. 0.2 mg C/L) between the column inlet and outlet for all temperatures could be related to the recalcitrant nature of the DOM. Previous results from column studies also did not show any temperature dependence of the DOM consumption after the first sampling point at a retention time of about one day (Grünheid et al., 2008). Moreover, the authors of field studies at river-infiltration systems observed a high correlation between oxygen consumption and temperature, but no correlation between DOM consumption and temperature (Brugger et al., 2001; Diem et al., 2013b).

(Fig. 4)

3.2.2 Kinetics of oxygen consumption

The measured oxygen concentration profiles for each temperature (5°C, 12.5°C, 20°C and 30°C) are shown in Fig. 5. The oxygen concentration of the feed water was 7.8 mg/L at 5.0°C, 12.5°C and 20.0°C and 7.0 mg/L at 30.0°C. Similarly to the previous experiments (see Section 3.1.1), the highest rates of the oxygen consumption could be observed at the column inlet (i.e., between SP0 and SP1) (Fig. 5).

(Fig. 5)

After the initial phase, the profiles of the oxygen concentration showed a nearly linear behavior, corresponding to zero-order kinetics (Fig. 5). This can be normally observed when the rate at which the growth-limiting nutrient becomes available is the rate-limiting step (Alexander, 1999). In our case, POM is assumed to be the primary electron donor for microbial respiration and hence for oxygen consumption. POM degradation involves hydrolytic reactions (Egli, 1995; Pusch et al., 1998) generating BDOM, which is subsequently oxidized to CO_2 by aerobic respiration. Fig. 6 shows a schematic representation of the processes involving POM hydrolysis (reaction 1) and BDOM oxidation (reaction 2), respectively. Oxygen and CO_2 in the aqueous solution enter the biofilm through diffusion. The hydrolytic reactions are commonly assumed to be the rate-limiting step for POM degradation (Valentini et al., 1997; Henze et al., 1999; Vavilin et al., 2008). Therefore, we hypothesize that the observed oxygen consumption rates for each temperature were mainly controlled by POM hydrolysis. This, together with the large POM reservoir identified in the column sand through the BOD measurements, explains well the observed pseudo-zero order reaction kinetics for the oxygen consumption in the column.

(Fig. 6)

The observed pseudo-zero order behavior also implies that the concentration of bacteria must be fairly constant over the length of the column (between SP1 and SP13). Bacterial densities were estimated indirectly by a protein assay conducted at the end of experiment 2.5 after column II was operated anaerobically for 66 days (see Section 2.3 for analytical methods). We expect that the protein content of the sand

samples from column II did not vary significantly after having changed the column operation mode from aerobic, which lasted 327 days, to anaerobic (66 days).

The protein content of the pristine sand was lower than the samples from the column, indicating that a significant bacterial growth occurred during the column experiments (Fig. 7). Nearly constant protein concentrations were measured in samples SP2-SP13 suggesting a uniform growth and distribution of bacteria through the column (Fig. 7). This implies that POM supporting bacterial growth was hydrolyzed at a constant rate throughout the column (i.e., after SP1), which is consistent with the observed pseudo-zero order reaction kinetics for the oxygen consumption. A higher protein concentration in sample SP1 compared with the average of SP2-SP13 ($p < 0.001$, Z-test statistics) may reflect bacterial growth by the presence of non-measurable BDOM near the column inlet (see Section 3.1.3).

(Fig. 7)

3.2.3 Temperature dependence of aerobic respiration: Activation energy

The oxygen consumption in the column has been shown to be associated with the degradation of POM present on the sand and to depend on temperature (Fig. 5). To quantify the observed temperature dependence, an Arrhenius-type approach, typical for chemical and biological reactions (Middelburg et al., 1996; Weston and Joye, 2005; Burdige, 2011), was applied (Eq. 2):

$$\ln(k(T)) = \ln(A) - \frac{E_a}{R} \cdot \frac{1}{T} \quad (2)$$

where $k(T)$ is the temperature-dependent reaction rate constant (in our case the observed pseudo zero-order oxygen consumption rate constant in Ms^{-1}), A the pre-exponential factor (in Ms^{-1}), E_a the apparent Arrhenius activation energy (in Jmol^{-1}), R

the universal gas constant (in $\text{Jmol}^{-1}\text{K}^{-1}$) and T the temperature (in K). Fig. 8 shows an Arrhenius-type plot of the data. Based on the good linearity ($r^2=0.97$), the apparent activation energy E_a can be determined from the slope $\left(\frac{E_a}{R}\right)$ of the straight line in Fig. 8, which results in a value of $\sim 70 \text{ kJmol}^{-1}$.

(Fig. 8)

The E_a value of $\sim 70 \text{ kJmol}^{-1}$ derived from our column experiments is consistent with a value of $51 \pm 12 \text{ kJmol}^{-1}$ ($n=94$) determined from measurements of benthic respiration over the temperature range $5\text{-}25^\circ\text{C}$ on stones collected from the Thur River (Acuna et al., 2008). Similar values of $54\text{-}125 \text{ kJmol}^{-1}$ (Middelburg et al., 1996) and $46\text{-}89 \text{ kJmol}^{-1}$ (Weston and Joye, 2005) were reported in studies of the temperature dependence of organic matter degradation in intertidal and marine sediments, respectively.

The activation energy for oxygen consumption can also be calculated from field observations of oxygen concentrations at, for example, the Thur River infiltration system (Diem et al., 2013a). In this study, the oxygen consumption rates were modeled with a temperature factor defined by a function with a maximum rate at 35°C (O'Connell, 1990) and with a discharge-dependent term. The activation energy for aerobic respiration during infiltration was estimated to be $\sim 63 \text{ kJmol}^{-1}$ over the temperature range $5\text{-}30^\circ\text{C}$ for low river discharges of $<20 \text{ m}^3/\text{s}$ (Diem et al., 2013a). This activation energy is similar to our experimentally derived activation energy ($\sim 70 \text{ kJmol}^{-1}$), showing a good agreement between the field-based model and our experimentally derived value.

3.2.4 Redox processes involving nitrogen species

The profiles of the oxygen concentration in Fig. 5 show that the oxygen consumption rate increased with increasing temperatures, leading to anoxic conditions at 30.0°C for residence times >7 h (i.e., at SP11, after 18 cm). To better characterize the redox milieu under such conditions, nitrate, nitrite and ammonium were measured in the column after an operation time of 18 days (Fig. 9). As soon as the oxygen concentration approached ≤ 0.1 mg/L, nitrite started to increase, reaching a maximum of 55 $\mu\text{g N/L}$ at a residence time of about 10 h (Fig. 9). Ammonium appeared at a residence time of about 8 h and did not reach a maximum. Nitrate showed a decreasing trend for residence times >8 h (i.e., at SP12, after 22 cm). These findings indicate that denitrification proceeded in the same section of the column where nitrite, an intermediate product of denitrification, was formed. This view was corroborated by the fact that ~30% of the nitrate decrease can be explained by the detected nitrite concentration. The remaining 70% of the nitrate lost might be explained by the formation of N_2 , or other denitrification products (e.g. N_2O). Formation of ammonium could be related to the anoxic degradation of nitrogen containing organic compounds, or to nitrate ammonification. The maximum detected nitrite concentration (55 $\mu\text{g N/L}$) is about one order of magnitude lower than the concentration recommended in the WHO guideline for drinking water (900 $\mu\text{g N/L}$) (WHO, 2011) and in a similar range as the value in the European guideline (150 $\mu\text{g N/L}$) (EU, 1998). Although the nitrite concentrations given in the WHO and EU guidelines are not exceeded under our experimental conditions, the formation of nitrite represents a potential threat for drinking water quality under such anoxic conditions.

(Fig. 9)

3.3 Mobilization of Mn(II) under oxygen- and nitrate-free conditions

Nitrate-free Thur River water stripped of oxygen was added as feed water to test whether Mn(III/IV)- and Fe(III)-reducing conditions could develop under this scenario. No Fe(II) could be measured in the entire column during this experiment, whereas Mn was mobilized as Mn(II) (Fig. 10a), suggesting that in the absence of oxygen and nitrate, Mn(III/IV)(hydr)oxides became terminal electron acceptors for the microorganisms.

According to the homogeneous POM distribution throughout the column and in analogy to aerobic respiration, we would have expected a constant reductive dissolution rate of Mn(III/IV)(hydr)oxides throughout the column leading to a steady Mn(II) increase between SP1-SP14, only limited by MnCO_3 solubility (for calculations, see Section 2.4). However, we observed a fast increase of Mn(II) near the column inlet (SP1-SP5) after 9, 16 and 27 days, followed by a decrease beyond SP8 (Fig. S2). This can also be observed in Fig. 10a, which shows the Mn(II) concentration as a function of the column operation time for each sampling port. Here, the Mn(II) concentration increased quickly for all sampling ports and peaked after ~7, ~14 and ~21 days for SP1, SP5 and SP8, respectively, approaching zero after that, whereas it reached MnCO_3 equilibrium for SP11 and SP14 (Fig. 10a).

We hypothesize that the fast Mn increase near the column inlet could be associated with a higher biological activity in this zone (see Section 3.2.2) and hence to a higher POM hydrolysis rate. From the experiments under aerobic conditions at 20°C (Fig. 1a and Fig. 5), we already observed a fast oxygen consumption at the column inlet (SP0-SP1) related to POM hydrolysis generating BDOM. In absence of oxygen and nitrate, part of this BDOM could propagate into the column and be available for Mn(III/IV) reduction. The decrease of the Mn(II) concentration beyond

SP8 (Fig. S2) could be due to adsorption processes of Mn(II) on e.g., Mn(III/IV)(hydr)oxide surfaces.

Furthermore, the Mn(II) concentration profiles in Fig. S2 are shifted towards the outlet with increasing operation time, possibly because of a depletion of Mn(III/IV)(hydr)oxides in the zone between SP1-SP8. To test this hypothesis, the reactive pools of Mn(III/IV)(hydr)oxides of the pristine and the column sand were quantified at the end of the experiment (after 66 days) with a buffered ascorbate solution at pH 7.1, according to Hyacinthe et al. (2006) (see Section 2.3). The amount of Mn(II) reduced by ascorbate in the pristine sand ($\sim 23 \mu\text{g/g}$ sand) was significantly higher than that in the column sand for all sampling ports, showing that a considerable part of the reactive Mn pool was consumed during the experiment (Fig. 10b). Lower Mn(II) sand concentrations were found at SP1 and SP5 compared to SP8, SP11 and SP14 (Fig. 10b). This is a confirmation of a partial depletion of the reactive pool of Mn(III/IV)(hydr)oxides at SP1 and SP5.

As a consequence of the initial depletion of the Mn pool, the extent of reductive dissolution rate of Mn(III/IV)(hydr)oxides decreased in the first section of the column (SP1-SP5) with increasing column operation time. This led to lower Mn(II) concentrations at SP1, SP5 and possibly SP8 (the Mn(II) concentration at SP8 reflects the accumulation of Mn(II) between SP1-SP8). For the sampling ports further in the column (SP8, SP11 and SP14), higher manganese concentrations in the sand were found (Fig. 10b), giving sufficient potential for a further increase of Mn(II) at SP11 and SP14. However, the Mn(II) concentrations at these sampling points were limited by the solubility of MnCO_3 .

Even though $\sim 75 \mu\text{g Fe/g}$ sand could be measured in the pristine sand by the ascorbate method (data not shown), Fe(II) could not be detected during the experiment. This suggests that conditions favorable for the reductive dissolution of

Fe(III)(hydr)oxides did not occur in our experimental system, but cannot be excluded at actual riverbank filtrations sites.

(Fig. 10)

3.4 Practical implications

Several studies have investigated the impact of climate change on groundwater quantity, but only a few have focused on processes affecting groundwater quality (Green et al., 2011). A recent review by Sprenger et al. (2011) evaluated the vulnerability of riverbank filtration systems to climate change considering two scenarios, drought and flood. Overall, increasing surface water temperatures are expected to favor anoxic/anaerobic conditions in the future (Sprenger et al., 2011), which is in line with our results (see Sections 3.2.2 and 3.2.4). High vulnerability for the drought scenario is projected for the DOM removal because of higher DOC concentrations in the source water and incomplete degradation under anaerobic conditions (Sprenger et al., 2011). The effects of the presumed increased DOC concentrations and altered DOM composition on the redox processes are however still unknown.

Currently, an upgrade of wastewater treatment plant effluents in Switzerland with ozonation (Joss et al., 2008; Zimmermann et al., 2011) or powdered activated carbon (Nowotny et al., 2007) is planned to reduce the discharge of organic micropollutants to the water bodies. Ozonation is usually followed by a sand filtration step, which effectively removes BDOM formed during ozonation (Zimmermann et al., 2011). Powdered activated carbon treatment reduces DOM by adsorption processes (Nowotny et al., 2007; Worch, 2010). Therefore, DOM loads from upgraded wastewater treatment plants into the receiving rivers are expected to be reduced in the

future, counteracting the smaller dilution, which would lead to higher DOC concentrations. In addition to that, our results showed that increasing DOC concentrations from wastewater effluent did not affect the redox processes in our experimental system (see Section 3.1.2). Based on the lower DOM input in rivers by polishing treatment of wastewater plant effluents and its subordinate role as an electron donor, only a minor effect of DOM on the development of anoxic conditions is expected during future summer conditions.

In the column experiments, a significant effect of the hydraulic residence time on the oxygen consumption and on the development of anoxic conditions was observed (see Section 3.1.4). At the same time, however, high hydraulic residence times are beneficial for the removal of microorganisms and pathogens (Sprenger et al., 2011). Since infectious diseases represent the most important health risks with respect to drinking water, removal of microorganisms and pathogens has absolute priority (WHO, 2011). The Swiss regulation for groundwater protection defines a minimum groundwater travel time of 10 days before abstraction, which allows for an adequate inactivation of microorganisms (Kunz et al., 2009). To determine the optimal residence time, which allows for good pathogen removal without the formation of anoxic conditions, site-specific information about the hydrogeological conditions and the redox parameters are needed, as also suggested by Schoenheinz and Grischek (2011).

Today, groundwater derived from riverbank filtration in Switzerland is generally oxic and denitrification is rarely observed. During future summer conditions, however, the effect of high temperatures ($\geq 20^{\circ}\text{C}$) over several weeks/months could lead to transient anoxic conditions. Complete denitrification was not observed in the present study, but cannot be excluded at actual riverbank filtration systems during future heat waves. Therefore, it will be essential to monitor oxygen and nitrogen species (nitrate,

nitrite and ammonium) at riverbank filtration systems especially during future heat waves.

The formation of ammonium could be problematic in the context of drinking water disinfection, since it can quickly react with chlorine leading to the formation of chloramines ($\text{HOCl} + \text{NH}_3 \rightarrow \text{NH}_2\text{Cl} + \text{H}_2\text{O}$), which lower the disinfection efficiency (Deborde and von Gunten, 2008). At Swiss riverbank filtration systems, such as the Thur River, disinfection is not practiced, but in cases where low chlorine doses are applied (e.g. $7 \mu\text{M Cl}_2$ or 0.5 mg/L Cl_2), the formation of ammonium in moderate concentrations ($<7 \mu\text{M NH}_4^+$) can substantially reduce the disinfection efficiency of chlorine.

4 Conclusion

Laboratory column experiments carried out with filtered river water were conducted to simulate the effect of temperature, DOM concentration/composition and flow rate on redox processes during riverbank filtration. The following conclusions can be drawn from our results:

1. Biodegradable dissolved organic matter (BDOM) was mainly removed immediately at the column inlet by aerobic respiration. This might lead to higher microbial concentrations near the infiltration zone at actual riverbank filtration systems even if BDOM is not measurable. DOM from wastewater treatment plant effluents did not enhance aerobic respiration and did not promote anoxic conditions in our laboratory columns.
2. Particulate organic matter (POM) associated with natural sand appears to be the main terminal electron donor in the infiltration process and can sustain aerobic

respiration for long periods. A POM limitation was not observed in the laboratory column system.

3. Low infiltration rates induce a higher oxygen consumption than higher rates for a certain infiltration distance, which could lead to anoxic conditions.

4. The aerobic respiration associated with POM degradation strongly depends on temperature with an activation energy of $\sim 70 \text{ kJmol}^{-1}$. Only a small fraction of the riverine DOM is easily degradable (i.e., BDOM) and its consumption does not seem to be sensitive to temperature.

5. At high temperatures (30°C), fully anoxic conditions were observed, with partial denitrification ($\sim 30\%$) and formation of nitrite and ammonium. Although nitrite concentrations were below WHO and EU drinking water guidelines in our experiments, this parameter should be monitored at actual riverbank filtration sites during future heat waves. If the produced water is chlorinated, the presence of ammonium could lead to a reduction in disinfection efficiency due to chloramine formation.

6. The combined action of high temperatures ($\geq 20^\circ\text{C}$) and low infiltration rates ($\leq 0.01 \text{ m/h}$) could lead to transient anoxic conditions during future summer conditions. Even under fully anoxic conditions, no complete denitrification was observed, so that nitrate acts as a redox buffer preventing the reductive dissolution of Mn(III/IV)(hydr)oxides.

7. Mn(II) was mobilized, whereas Fe(II) was not mobilized in absence of oxygen and nitrate, but Fe(III)-reduction cannot be excluded at actual riverbank filtration systems under these conditions.

Acknowledgements

This study was accomplished within the National Research Program “Sustainable Water Management” (NRP61) and funded by the Swiss National Science Foundation (SNF, Project No. 406140-125856). We would like to thank the AuA Laboratory, Elisabeth Salhi, Irene Brunner, Thomas Fleischmann and Stefan Koetzsch for the analytical support and Peter Gäumann and his workshop-team for constructing the columns. Moreover, we would like to express our gratitude to Samuel Diem, Fabian Soltermann, Sabrina Bahnmüller, Eduard Hoehn and Jacqueline Taber for helpful discussions.

References

- Acuna, V., Wolf, A., Uehlinger, U., Tockner, K., 2008. Temperature dependence of stream benthic respiration in an Alpine river network under global warming. *Freshwater Biol.* 53 (10), 2076-2088.
- Alexander, M., 1999. Biodegradation and bioremediation. Academic Press, San Diego.
- Bourg, A.C.M., Bertin, C., 1993. Biogeochemical processes during the infiltration of river water into an alluvial aquifer. *Environ. Sci. Technol.* 27 (4), 661-666.
- Brugger, A., Wett, B., Kolar, I., Reitner, B., Herndl, G.J., 2001. Immobilization and bacterial utilization of dissolved organic carbon entering the riparian zone of the alpine Enns River, Austria. *Aquat. Microb. Ecol.* 24 (2), 129-142.
- Burdige, D.J., 2011. Temperature dependence of organic matter remineralization in deeply-buried marine sediments. *Earth Planet. Sc. Lett.* 311 (3-4), 396-410.
- CH2011, 2011. Swiss Climate Change Scenarios CH2011. C2SM, MeteoSwiss, ETH, NCCR Climate and OcCC, Zurich, pp. 88.

- Deborde, M., von Gunten, U., 2008. Reactions of chlorine with inorganic and organic compounds during water treatment-Kinetics and mechanisms: A critical review. *Water Res.* 42 (1-2), 13-51.
- Diem, S., Cirpka, O.A., Schirmer, M., 2013a. Modeling the dynamics of oxygen consumption upon riverbank filtration by a stochastic-convective approach. *J. Hydrol.* 505, 352-363.
- Diem, S., Rudolf von Rohr, M., Hering, J.G., Kohler, H.P.E., Schirmer, M., von Gunten, U., 2013b. NOM degradation during river infiltration: Effects of the climate variables temperature and discharge. *Water Res.* 47 (17), 6585-6595.
- DIN, 1983a. Deutsche Einheitsverfahren zur Wasser-, Abwasser- und Schlammuntersuchung, Bestimmung des Ammonium-Stickstoffs (E5), Teil 5, DIN 38406. Deutsches Institut für Normung DIN, pp. 1-6.
- DIN, 1983b. Deutsche Einheitsverfahren zur Wasser-, Abwasser- und Schlammuntersuchung, Bestimmung von Mangan (E2), Teil 2, DIN 38406. Deutsches Institut für Normung DIN, pp. 1-8.
- DIN, 1993. Deutsche Norm zur Bestimmung von Nitrit, EN 26777. Deutsches Institut für Normung DIN, pp. 1-11.
- Doussan, C., Poitevin, G., Ledoux, E., Delay, M., 1997. River bank filtration: Modelling of the changes in water chemistry with emphasis on nitrogen species. *J. Contam. Hydrol.* 25 (1-2), 129-156.
- Egli, T., 1995. The ecological and physiological significance of the growth of heterotrophic microorganisms with mixtures of substrates. In: Jones, G.N. (Ed.), *Advances in Microbial Ecology*. Plenum Press, New York, pp. 305-386.
- EU, 1998. European Union (EU) Council Directive 98/83/EC of 3 November 1998 on the quality of water intended for human consumption.
- FOEN, 2012. Effects of Climate Change on Water Resources and Watercourses. Synthesis Report on the "Climate Change and Hydrology in Switzerland" (CCHydro) Project. Federal Office for the Environment FOEN, Bern, pp. 76.

- 730 Green, T.R., Taniguchi, M., Kooi, H., Gurdak, J.J., Allen, D.M., Hiscock, K.M., Treidel, H.,
 731 Aureli, A., 2011. Beneath the surface of global change: Impacts of climate change on
 732 groundwater. *J. Hydrol.* 405 (3-4), 532-560.
- 733 Greskowiak, J., Prommer, H., Massmann, G., Nützmann, G., 2006. Modeling seasonal redox
 734 dynamics and the corresponding fate of the pharmaceutical residue phenazone during
 735 artificial recharge of groundwater. *Environ. Sci. Technol.* 40 (21), 6615-6621.
- 736 Grischek, T., Hiscock, K.M., Metschies, T., Dennis, P.F., Nestler, W., 1998. Factors affecting
 737 denitrification during infiltration of river water into a sand and gravel aquifer in Saxony,
 738 Germany. *Water Res.* 32 (2), 450-460.
- 739 Grünheid, S., Amy, G., Jekel, M., 2005. Removal of bulk dissolved organic carbon (DOC) and
 740 trace organic compounds by bank filtration and artificial recharge. *Water Res.* 39 (14),
 741 3219-3228.
- 742 Grünheid, S., Huebner, U., Jekel, M., 2008. Impact of temperature on biodegradation of bulk
 743 and trace organics during soil passage in an indirect reuse system. *Water Sci. Technol.*
 744 57 (7), 987-994.
- 745 Hannappel, S., Scheibler, F., Huber, A., Sprenger, C., 2014. Characterization of European
 746 managed aquifer recharge (MAR) sites - Analysis. EU project Demeau, M11.1, pp 51.
- 747 Henze, M., Gujer, W., Mino, T., Matsuo, T., Wentzel, M.C., Marais, G.V.R., Van Loosdrecht,
 748 M.C.M., 1999. Activated Sludge Model No.2d, ASM2d. *Water Sci. Technol.* 39 (1), 165-
 749 182.
- 750 Herbert, D., Phipps, P.J., Strange, R.E., 1971. Chemical Analysis of Microbial Cells (Chapter
 751 III). In: *Methods In Microbiology*, Volume 5, Part B. Edited by J.R. Norris and D.W.
 752 Ribbons. Academic Press. .
- 753 Hoehn, E., Scholtis, A., 2011. Exchange between a river and groundwater, assessed with
 754 hydrochemical data. *Hydrol. Earth Syst. Sc.* 15 (3), 983-988.
- 755 Huntscha, S., Rodriguez Velosa, D.M., Schroth, M.H., Hollender, J., 2013. Degradation of
 756 Polar Organic Micropollutants during Riverbank Filtration: Complementary Results from

- 757 Spatiotemporal Sampling and Push–Pull Tests. *Environ. Sci. Technol.* 47 (20), 11512-
758 11521.
- 759 Hyacinthe, C., Bonneville, S., Van Cappellen, P., 2006. Reactive iron(III) in sediments:
760 Chemical versus microbial extractions. *Geochim. Cosmochim. Acta* 70 (16), 4166-
761 4180.
- 762 Jacobs, L.A., von Gunten, H.R., Keil, R., Kuslys, M., 1988. Geochemical changes along a
763 river-groundwater infiltration flow path: Glattfelden, Switzerland. *Geochim. Cosmochim.*
764 *Acta* 52 (11), 2693-2706.
- 765 Joss, A., Siegrist, H., Ternes, T.A., 2008. Are we about to upgrade wastewater treatment for
766 removing organic micropollutants? *Water Sci. Technol.* 57 (2), 251-255.
- 767 Kedziorek, M.A.M., Geoffriau, S., Bourg, A.C.M., 2008. Organic matter and modeling redox
768 reactions during river bank filtration in an alluvial aquifer of the Lot River, France.
769 *Environ. Sci. Technol.* 42 (8), 2793-2798.
- 770 Kuehn, W., Mueller, U., 2000. Riverbank filtration: An overview. *J. Am. Water Works Ass.* 92
771 (12), 60-69.
- 772 Kunz, Y., von Gunten, U., Maurer, M., 2009. Wasserversorgung 2025 - Vorprojekt. Eawag, pp.
773 198.
- 774 Maeng, S.K., Sharma, S.K., Magic-Knezev, A., Amy, G., 2008. Fate of effluent organic matter
775 (EfOM) and natural organic matter (NOM) through riverbank filtration. *Water Sci.*
776 *Technol.* 57 (12), 1999-2007.
- 777 Massmann, G., Greskowiak, J., Dunnbier, U., Zuehlke, S., Knappe, A., Pekdeger, A., 2006.
778 The impact of variable temperatures on the redox conditions and the behaviour of
779 pharmaceutical residues during artificial recharge. *J. Hydrol.* 328 (1-2), 141-156.
- 780 Matsunaga, T., Karametaxas, G., von Gunten, H.R., Lichtner, P.C., 1993. Redox chemistry of
781 iron and manganese minerals in river-recharged aquifers: A model interpretation of a
782 column experiment. *Geochim. Cosmochim. Acta* 57 (8), 1691-1704.

- 783 Middelburg, J.J., Klaver, G., Nieuwenhuize, J., Wielemaker, A., De Haas, W., Vlug, T., Van
 784 Der Nat, J.F.W.A., 1996. Organic matter mineralization in intertidal sediments along an
 785 estuarine gradient. *Mar. Ecol.-Prog. Ser.* 132 (1-3), 157-168.
- 786 Mouchet, P., 1992. From conventional to biological removal of iron and manganese in France.
 787 *J. Am. Water Works Ass.* 84 (4), 158-167.
- 788 Mueller, B., 2004. ChemEQL, V.3.0, a program to calculate chemical speciation and chemical
 789 equilibria, Eawag.
- 790 Müller, R., Widemann, O., 1955. Die Bestimmung des Nitrat-Ions im Wasser. *Vom Wasser* 22,
 791 247-271.
- 792 Nowotny, N., Epp, B., von Sonntag, C., Fahlenkamp, H., 2007. Quantification and modeling of
 793 the elimination behavior of ecologically problematic wastewater micropollutants by
 794 adsorption on powdered and granulated activated carbon. *Environ. Sci. Technol.* 41
 795 (6), 2050-2055.
- 796 O'Connell, A.M., 1990. Microbial decomposition (respiration) of litter in eucalypt forests of
 797 South-Western Australia: An empirical model based on laboratory incubations. *Soil*
 798 *Biol. Biochem.* 22 (2), 153-160.
- 799 OECD, 1992. OECD Guideline for Testing of Chemicals, Guideline 301 D. Organisation for
 800 Economic Co-operation and Development OECD pp. 62.
- 801 Peter, S., Koetzsch, S., Traber, J., Bernasconi, S.M., Wehrli, B., Durisch-Kaiser, E., 2012.
 802 Intensified organic carbon dynamics in the ground water of a restored riparian zone.
 803 *Freshwater Biol.* 57 (8), 1603-1616.
- 804 Pusch, M., Fiebig, I., Brettar, H., Eisenmann, H., Ellis, B.K., Kaplan, L.A., Lock, M.A., Naegeli,
 805 M.W., Traunspurger, W., 1998. The role of micro-organisms in the ecological
 806 connectivity of running waters. *Freshwater Biol.* 40 (3), 453-495.
- 807 Scheurer, M., Michel, A., Brauch, H.J., Ruck, W., Sacher, F., 2012. Occurrence and fate of the
 808 antidiabetic drug metformin and its metabolite guanylurea in the environment and
 809 during drinking water treatment. *Water Res.* 46 (15), 4790-4802.

- Schmidt, C.K., Lange, F.T., Brauch, H.J., 2007. Characteristics and evaluation of natural attenuation processes for organic micropollutant removal during riverbank filtration. *Wat. Sci. Technol.* 7 (3), 1-7.
- Schoenheinz, D., Grischek, T., 2011. Behavior of dissolved organic Carbon during bank filtration under extreme climate conditions. *NATO Science for Peace and Security Series C: Environmental Security* 103, 51-67.
- Smith, P.K., Krohn, R.I., Hermanson, G.T., 1985. Measurement of protein using bicinchoninic acid. *Anal. Biochem.* 150 (1), 76-85.
- Sobczak, W.V., Findlay, S., 2002. Variation in bioavailability of dissolved organic carbon among stream hyporheic flowpaths. *Ecology* 83 (11), 3194-3209.
- Sprenger, C., Lorenzen, G., Hulshoff, I., Grutmacher, G., Ronghang, M., Pekdeger, A., 2011. Vulnerability of bank filtration systems to climate change. *Sci. Total Environ.* 409 (4), 655-663.
- Storck, F.R., Schmidt, C.K., Wülser, R., Brauch, H.J., 2012. Effects of boundary conditions on the cleaning efficiency of riverbank filtration and artificial groundwater recharge systems regarding bulk parameters and trace pollutants. *Water Sci. Technol.* 66 (1), 138-144.
- Stumm, W., Morgan, J.J., 1996. *Aquatic Chemistry. Chemical Equilibria and Rates in Natural Waters*, Third Edition. Wiley-interscience, New York.
- Tufenkji, N., Ryan, J.N., Elimelech, M., 2002. Bank filtration. *Environ. Sci. Technol.* 36 (21), 423-428.
- Valentini, A., Garuti, G., Rozzi, A., Tilche, A., 1997. Anaerobic degradation kinetics of particulate organic matter: A new approach. *Water Sci. Technol.* 36 (6-7), 239-246.
- Vavilin, V.A., Fernandez, B., Palatsi, J., Flotats, X., 2008. Hydrolysis kinetics in anaerobic degradation of particulate organic material: An overview. *Waste Management* 28 (6), 939-951.

- Vogler, P., 1965. Beiträge zur Phosphatanalytik in der Limnologie. II. Die Bestimmung des gelösten Ortophosphates. Fortschritte der Wasserchemie und ihrer Grenzgebiete 2, 109-119.
- von Gunten, H.R., Karametaxas, G., Krähenbühl, U., Kuslys, M., Giovanoli, R., Hoehn, E., Keil, R., 1991. Seasonal biogeochemical cycles in riverborne groundwater. *Geochim. Cosmochim. Acta* 55 (12), 3597-3609.
- von Gunten, U., Zobrist, J., 1993. Biogeochemical changes in groundwater-infiltration systems: Column studies. *Geochim. Cosmochim. Acta* 57 (16), 3895-3906.
- Weston, N.B., Joye, S.B., 2005. Temperature-driven decoupling of key phases of organic matter degradation in marine sediments. *P. Natl. Acad. Sci. USA* 102 (47), 17036-17040.
- WHO, 2011. Guidelines for Drinking-water Quality, Fourth Edition. World Health Organization WHO, pp. 541.
- Worch, E., 2010. Competitive adsorption of micropollutants and NOM onto activated carbon: Comparison of different model approaches. *J. Water Supply Res. T.* 59 (5), 285-297.
- Zimmermann, S.G., Wittenwiler, M., Hollender, J., Krauss, M., Ort, C., Siegrist, H., von Gunten, U., 2011. Kinetic assessment and modeling of an ozonation step for full-scale municipal wastewater treatment: Micropollutant oxidation, by-product formation and disinfection. *Water Res.* 45 (2), 605-617.

Figure captions

Fig. 1. (a) Profiles of the relative oxygen concentration (normalized to the values at SP0) and (b) pH for “DOM-free” Thur River water (n=3) (○), Thur River water (n=1) (◆), Thur River water/effluent mixtures (*average of four mixtures: 90/10, 80/20, 70/30, 60/40%) (□) and Thur River water amended with 1.75 mg C/L sodium acetate (n=3) (△). The first data point corresponds to the sampling port at the inlet (SP0), the last data point to the sampling port at the outlet of the column (SP14) for each experiment. Mean values and standard deviations are shown as symbols and error bars, respectively.

Fig. 2. Net biological oxygen demand (BOD) of the pristine sand (mg oxygen/mg sand) determined in individual batch experiments conducted for 5, 7, 14, 21 and 28 days. Mean values (n=2) are shown corrected for the blank associated with oxygen uptake by the inoculum; Error of measurement is $<1 \times 10^{-5}$ mg O₂ / mg sand.

Fig. 3. Profiles of the relative oxygen concentration (normalized to the values at SP1) as a function of (a) infiltration distance and (b) residence time at flow rates of 0.10 (n=1), 0.20 (n=1), 0.33 (n=1) and 1.00 (n=13) mL/min at 20°C. Mean values and standard deviations (for 1 mL/min) are shown as symbols and error bars, respectively.

Fig. 4. Total average oxygen and DOM (as DOC) consumption in column experiments between SP0 and SP14. Standard deviations are shown as error bars (n=3).

Fig. 5. Measured oxygen concentration profiles (symbols) and least-squares linear regression lines at 5.0, 12.5, 20.0 and 30.0°C at a flow rate of 0.3 mL/min. Mean

values and standard deviations are shown as symbols and error bars, respectively (n=3).

Fig. 6. Schematic representation of oxygen consumption associated with degradation of POM on sand grains. Reaction (1) represents POM hydrolysis and reaction (2) BDOM oxidation.

Fig. 7. Protein concentration (expressed as bovine serum albumin concentration, BSA) of the sand from column II (SP1, SP2, SP3, SP5, SP8, SP9, SP10, SP11, SP12, SP13) (●) measured after 393 days of operation (Table 2, end of experiment 2.5) and of pristine sand (dashed line). The dotted lines represent the errors of measurement for the pristine sand (n=3). Mean values and standard deviations are shown as symbols and error bars, respectively (n=3).

Fig. 8. Arrhenius-type correlation between the rate constant ($\ln(k)$) for oxygen consumption and $\frac{1}{T}$. The symbols represent the experimental data at 30.0, 20.0, 12.5 and 5.0°C (n=3) (Fig. 5), the line shows a least-squares linear regression.

Fig. 9. Measured oxygen (---), nitrate (◇), nitrite (△) and ammonium (●) concentrations after 18 days of operation of column II at 30.0°C at a flow rate of 0.3 mL/min (Table 2, experiment 2.1). Mean values and standard deviations (for nitrate) are shown as symbols and error bars, respectively (n=3). For nitrate, nitrite and ammonium, lines help to guide the reader's eye.

913 Fig. 10. (a) Mn(II) concentration at SP0 (●), SP1 (○), SP5 (▼), SP8 (△), SP11 (■) and
914 SP14 (□) as a function of the column operation time at 20°C and at a flow rate of 0.3
915 mL/min. The Mn(II) concentration in equilibrium with rhodochrosite (MnCO_3) is shown
916 by the dashed line (for calculations, see Section 2.4). (b) Average amount of Mn
917 reduced [$\mu\text{g/g}$ sand] by ascorbate in the pristine (dashed line) and in the sand from
918 column II (circles) (SP1, SP5, SP8, SP11 and SP13) after 66 days of operation. For
919 the pristine sand, an average of three samples after 0.5, 1, and 2.5 hours equilibration
920 with the ascorbate solution is shown with the errors of measurement (dotted lines), for
921 the column II samples, an average of samples after 0.5, 1, and 2.5 hours equilibration
922 is shown together with the corresponding standard deviations.

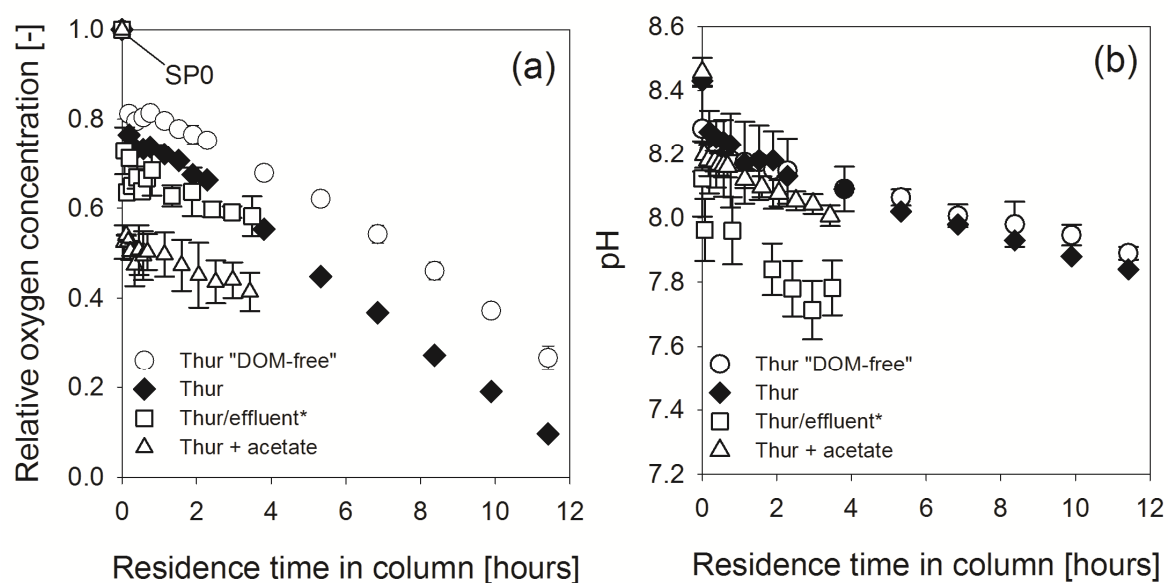
Table 1. Hydraulic characteristics of the columns (effective porosity, dispersivity and total pore volume) and sand mass present in the columns. The effective porosity and the dispersivity were calculated with the program CXTFIT (Toride et al., 1995) using the electrical conductivity data.

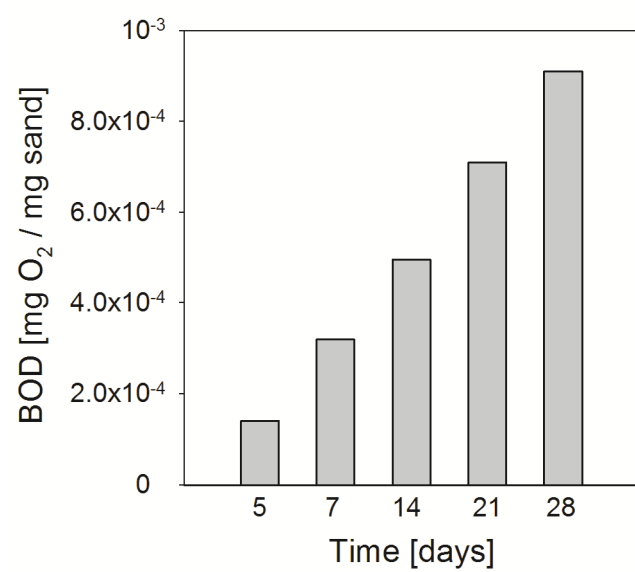
	Column I	Column II
Effective porosity [-]	0.38	0.32
Dispersivity [cm]	0.1	0.1
Total pore volume [mL]	245	206
Sand mass [g]	885	876

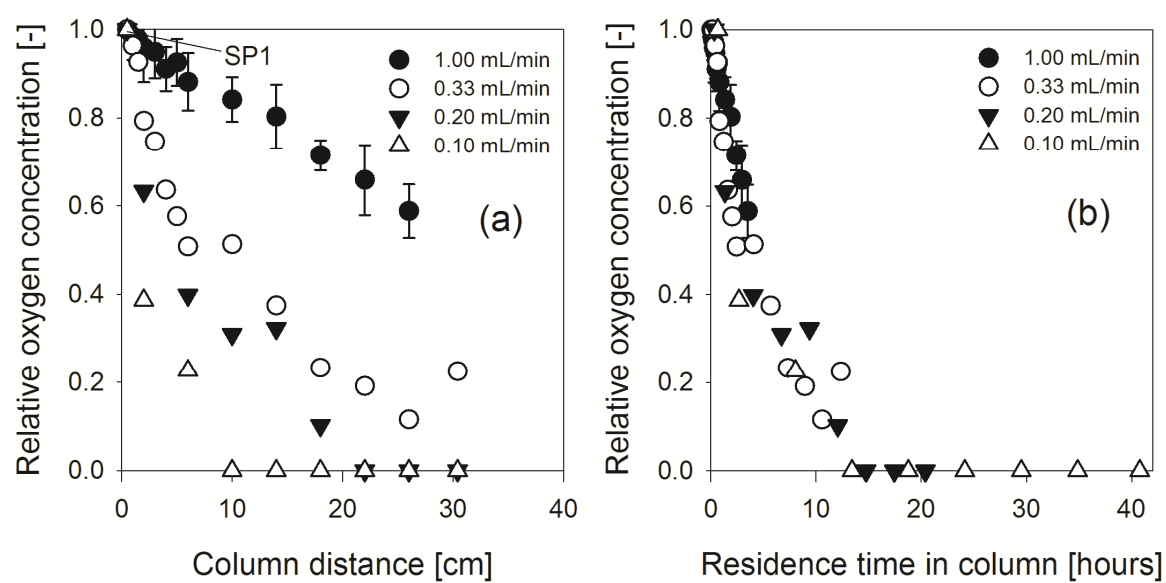
Table 2. Operational conditions of all column experiments, which are listed in a chronological order for columns I (1.1, 1.2) and II (2.1-2.5). Experiments 1.2, 2.1 and 2.2 were conducted with unaltered Thur River water as feed water.

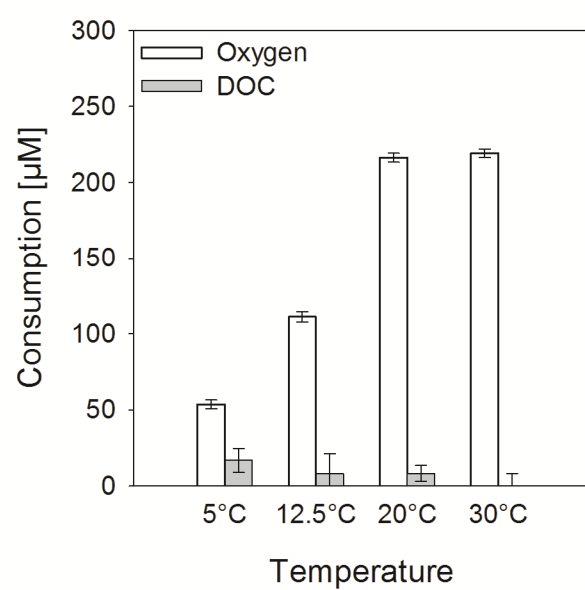
Experiment	Flow rate [mL/min] ([m/h])	Residence time [h]	Temperature [°C]	Column
(1.1) Thur River water/effluent mixtures ^a	1.0 (0.07)	4	22	I
(1.2) Variation of flow rate	0.1 (0.007), 0.2 (0.01)	40, 20	20	I
	0.33 (0.02), 1.0 (0.07)	12, 4		
(2.1) Variation of temperature	0.3 (0.03)	11.5	5, 12.5, 20, 30	II
(2.2) Thur River water	0.3 (0.03)	11.5	20	II
(2.3) Addition of "DOM-free" Thur River water	0.3 (0.03)	11.5	20	II
(2.4) Addition of acetate	1.0 (0.09)	3.5	20	II
(2.5) Addition of oxygen- and nitrate-free Thur River water	0.3 (0.03)	11.5	20	II

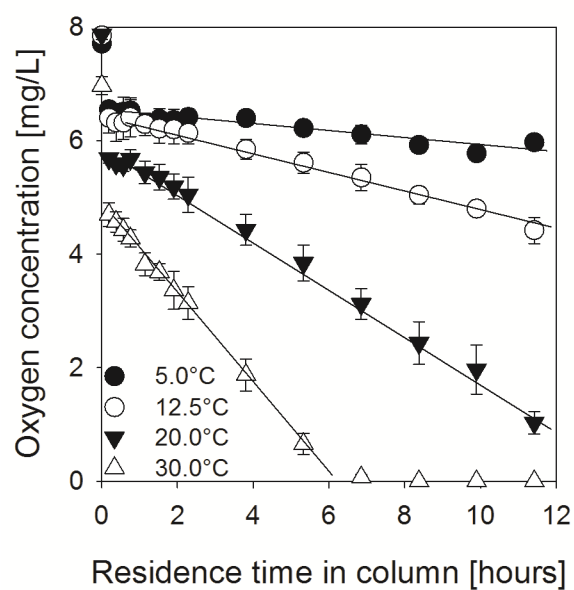
^a 90/10, 80/20, 70/30, 60/40%

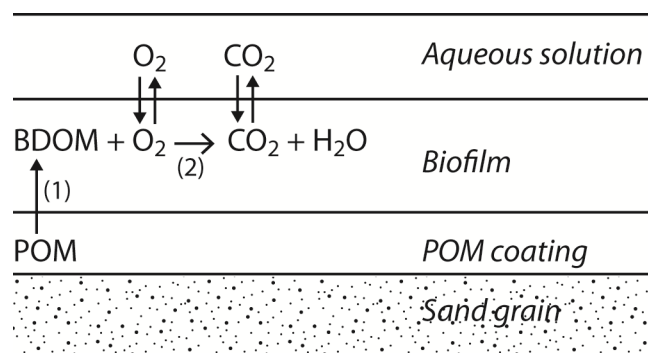


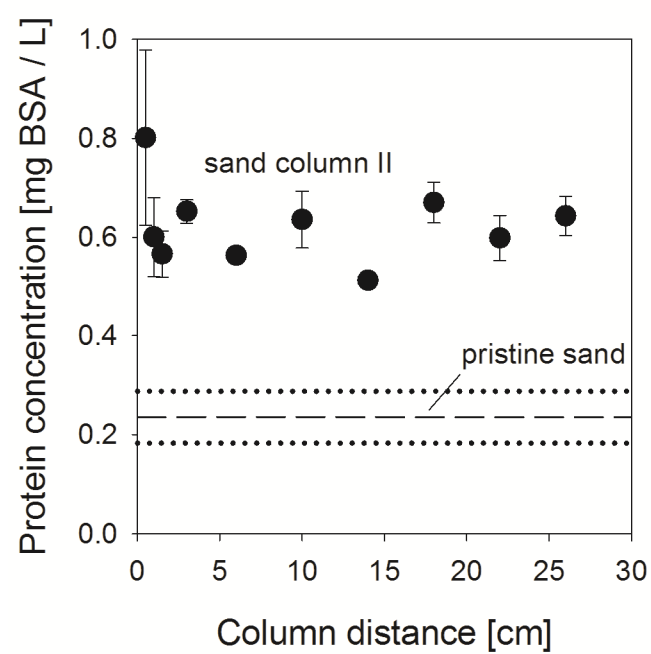


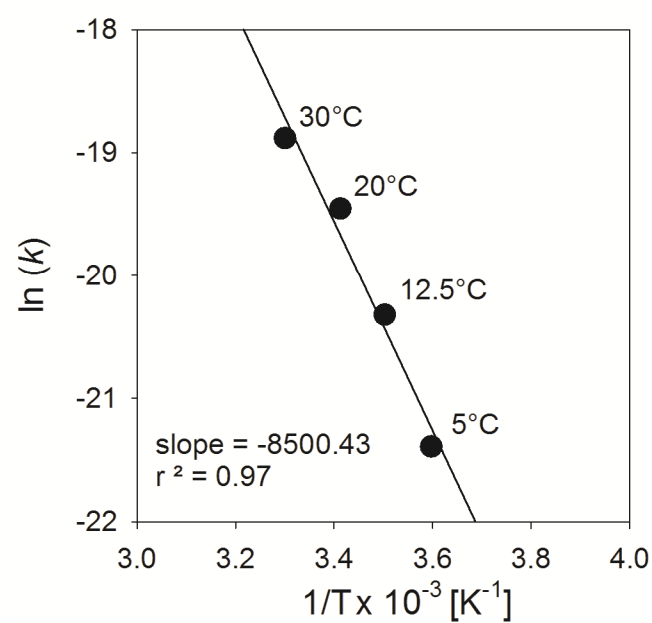


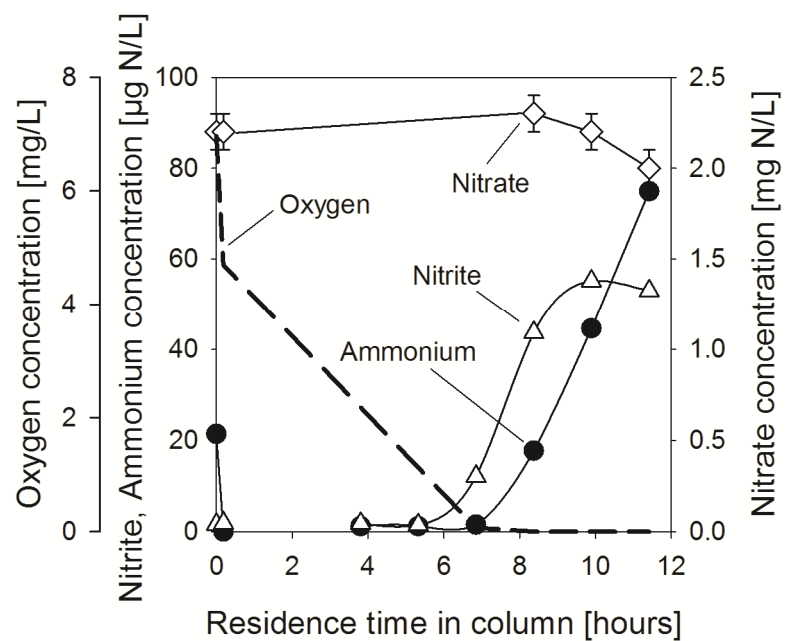


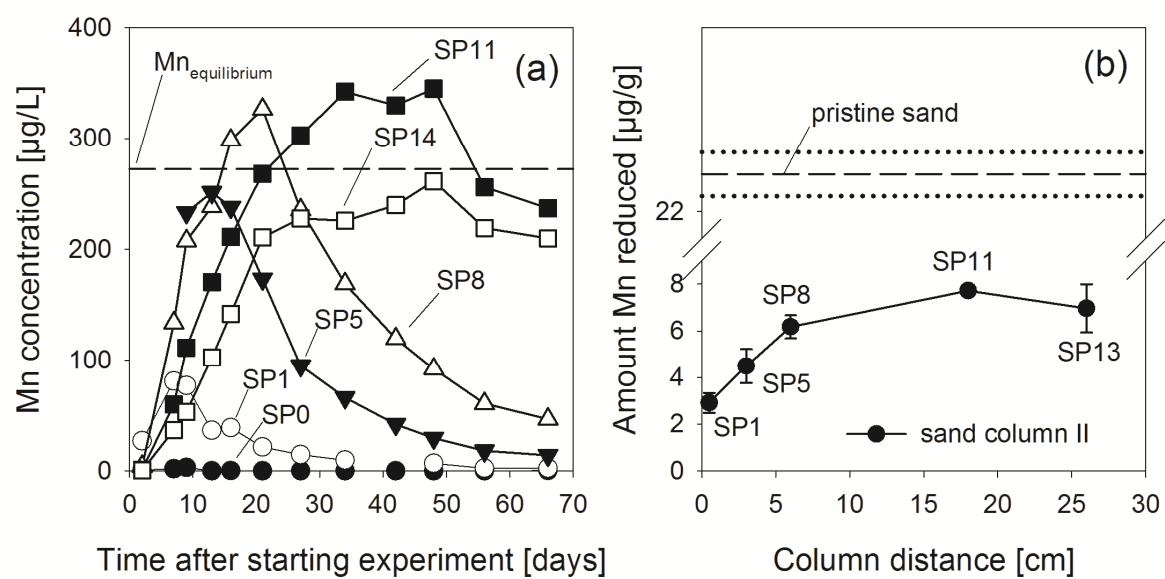












Supporting information for

Column studies to assess the effects of climate variables on redox processes during riverbank filtration

Matthias Rudolf von Rohr^{1,2}, Janet G. Hering^{1,2,3}, Hans-Peter E. Kohler^{1,2}, Urs von Gunten^{1,2,3,*}

¹ EAWAG, Swiss Federal Institute of Aquatic Science and Technology, Water

Resources & Drinking Water, Überlandstrasse 133, 8600 Dübendorf, Switzerland

² ETH Zürich, Institute of Biogeochemistry and Pollutant Dynamics, Universitätstrasse 16, 8092 Zürich, Switzerland

³ Ecole Polytechnique Fédérale de Lausanne (EPFL), School of Architecture, Civil and Environmental Engineering (ENAC), 1015 Lausanne, Switzerland

*Corresponding author

Urs von Gunten

Überlandstrasse 133

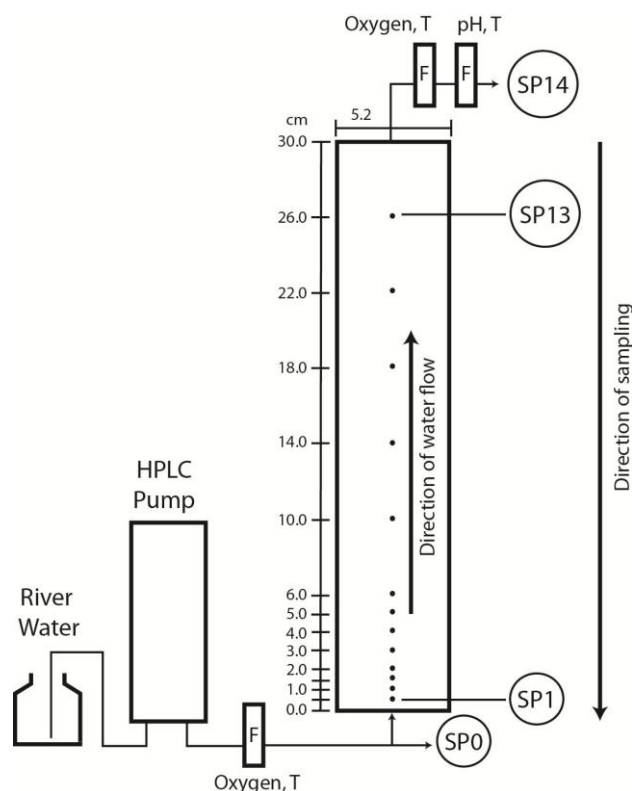
P.O. Box 611

Phone: +41 58 765 5270

Fax: +41 58 765 5210

urs.vongunten@eawag.ch

29



30

31 Fig. S1. Set-up of the column system, in which river water was pumped by a HPLC-
 32 pump from the bottom to the top of the column. The column was equipped with 13
 33 sampling ports (SP1-13), one sampling port was installed before (SP0) and one after
 34 (SP14) the column. Oxygen, temperature (T) and pH were measured in flow-through
 35 cells (F). Samples were taken in counter current mode from top to bottom during
 36 sampling events. Modified from Diem et al., 2013.

37

38

39

40

Table S1. Composition of feed waters used for the column experiments. Thur River waters were collected at the Thur River field site (Diem et al., 2013). Treated wastewater effluent (called effluent) was collected at the wastewater treatment plant Dübendorf Neugut.

Experiment	Feed water and sampling date (day/month/year)	DOC mg C/L	Alkalinity mM	pH	NO ₂ ⁻ µg N/L	NH ₄ ⁺ µg N/L	NO ₃ ⁻ mg N/L	Cl ⁻ mg/L	SO ₄ ²⁻ mg/L	Na ⁺ mg/L	K ⁺ mg/L	Ca ²⁺ mg/L	Mg ²⁺ mg/L	PO ₄ ³⁻ µg P/L
(1.1) Thur River water/effluent mixtures (%/%)	Thur River water/effluent mixtures													
90/10	10.08.2011/11.07.2011	2.6	4.3	8.0	3.8	5.2	1.4	9.6	9.6	11.5	2.0	67.5	11.2	42.1
80/20	10.08.2011/29.08.2011	3.0	4.1	8.0	3.6	5.2	1.3	9.3	14.2	17.2	2.2	59.8	9.9	40.4
70/30	10.08.2011/29.08.2011	3.5	3.9	8.0	3.5	3.3	1.2	8.7	20.0	25.8	2.6	52.3	8.7	55.5
60/40	10.08.2011/13.09.2011	3.9	3.7	8.0	3.2	2.8	1.0	8.2	24.2	32.0	2.9	44.8	7.4	61.5
(1.2) Variation of flow rate	Thur River water													
1.0	16.02.2011	2.1	4.8	8.0	29.4	85.0	3.4	26.0	13.1	16.5	3.1	78.9	16.8	18.8
	24.03.2011	2.2	4.6	8.0	12.5	56.2	2.6	18.2	10.4	11.8	2.5	73.7	13.9	26.1
	20.04.2011	2.0	4.2	8.0	32.0	14.3	2.9	24.5	12.5	16.9	3.0	72.9	14.3	32.5
0.33	08.11.2011	2.4	5.0	8.0	3.7	<5.0	3.6	38.0	17.5	27.3	4.9	80.5	16.6	32.2
0.1, 0.2	06.02.2012	1.7	5.5	8.0	43.0	54.4	3.6	39.0	13.0	18.4	3.1	94.4	18.2	38.6
(2.1) Variation of temperature	Thur River water													
	13.08.2012	2.3	3.8	8.6	9.1	19.0	2.1	25.2	14.0	18.2	3.6	58.9	13.7	14.3
(2.2) Thur River water	Thur River water													
	26.09.2012	2.5	4.6	8.4	2.9	5.5	1.7	11.8	8.0	8.1	2.3	71.2	12.3	26.0
(2.3) Addition of "DOM-free" Thur River water	Treated Thur River water													
	26.09.2012	0.1	4.2	8.3	3.6	6.8	1.4	11.7	7.9	8.2	2.4	66.0	13.0	30.3
(2.4) Addition of acetate	Thur River water													
	07.02.2013	4.2	4.9	8.5	11.0	38.2	2.6	30.2	8.0	20.0	1.8	78.0	13.7	30.7
(2.5) Addition of oxygen- and nitrate-free Thur River water	Treated Thur River water													
	08.03.2013	2.1	4.5	8.4			0.1	138.1	7.0	98.2	<1.0	63.9	10.9	

Table S2. Composition of effluent before and after treatment with electrodialysis.

Effluent treatment with electrodialysis	DOC mg C/L	Alkalinity mM	NO ₂ ⁻ µg N/L	NH ₄ ⁺ µg N/L	NO ₃ ⁻ mg N/L	Cl ⁻ mg/L	SO ₄ ²⁻ mg/L	Na ⁺ mg/L	K ⁺ mg/L	Ca ²⁺ mg/L	Mg ²⁺ mg/L	PO ₄ ³⁻ µg P/L
Effluent 11.07.2011	4.9	4.4	4.8	14.8	7.2	68.9	31.6	68.1	9.7	69.8	10.6	88.0
After electrodialysis	4.9	1.7	<1.0	9.6	0.3	4.0	30.8	47.9	2.1	3.0	0.8	83.0
Effluent 29.08.2011	5.4	5.4	18.0	22.8	7.7	94.4	42.3	79.2	12.8	91.3	15.0	54.6
After electrodialysis	5.5	2.0	1.1	7.0	0.3	5.5	41.7	56.6	2.8	<5.0	<2.5	51.9
Effluent 13.09.2011	6.4	6.5	16.6	13.2	9.8	129.5	51.0	111.6	17.7	96.5	17.0	103.0
After electrodialysis	6.2	2.4	1.7	<5.0	0.3	5.2	50.0	68.8	4.1	<5.0	<2.5	98.0

Table S3. Composition of Thur River water collected on 26.09.2012 before and after treatment with 500 mg/L powdered activated carbon (PAC) (Norit W15 powdered activated carbon, NORIT Deutschland GmbH, Riesbürg, Germany).

River water treatment with PAC	DOC mg C/L	Alkalinity mM	NO ₂ ⁻ µg N/L	NH ₄ ⁺ µg N/L	NO ₃ ⁻ mg N/L	Cl ⁻ mg/L	SO ₄ ²⁻ mg/L	Na ⁺ mg/L	K ⁺ mg/L	Ca ²⁺ mg/L	Mg ²⁺ mg/L	PO ₄ ³⁻ µg P/L
River water	2.5	4.6	2.9	5.5	1.7	11.8	8.0	8.1	2.3	71.2	12.3	26.0
After treatment with PAC	0.1	4.2	3.6	6.8	1.4	11.7	7.9	8.2	2.4	66.0	13.0	30.3

Table S4. Composition of Thur River water collected on 08.03.2013 before and after treatment with electrodialysis and re-mineralization by addition of NaHCO₃ (300 mg/L final concentration), CaCl₂ x 6 H₂O (350 mg/L final concentration) and MgCl₂ x 6 H₂O (85 mg/L final concentration).

River water treatment with electrodialysis	DOC mg C/L	Alkalinity mM	NO ₂ ⁻ µg N/L	NH ₄ ⁺ µg N/L	NO ₃ ⁻ mg N/L	Cl ⁻ mg/L	SO ₄ ²⁻ mg/L	Na ⁺ mg/L	K ⁺ mg/L	Ca ²⁺ mg/L	Mg ²⁺ mg/L	PO ₄ ³⁻ µg P/L
River water	2.2	4.0	9.5	8.2	2.3	14.1	7.0	8.4	1.8	63.7	11.3	14.0
After electrodialysis	2.1	1.0			0.1	1.1	7.0	16.8	<1.0	<5.0	<2.5	
After electrodialysis and re-mineralization	2.1	4.5			0.1	138.1	7.0	98.2	<1.0	63.9	10.9	

Table S5. Mn(II) speciation in the column calculated by the chemical equilibrium modeling program ChemEQL V3.0 (Mueller, 2004). The initial Mn^{2+} concentration was calculated by the solubility product of rhodochrosite (MnCO_3) ($\text{Mn}^{2+} + \text{CO}_3^{2-} = \text{MnCO}_3$; $\log K = -10.39$, (Stumm and Morgan, 1996)) at pH 8.2 (for calculations, see Section 2.4). The main Mn(II) species are Mn^{2+} and MnCO_3 (aq) (highlighted in rectangles).

Species	Concentration [M]
Ca^{2+}	1.60×10^{-3}
CaOH^+	4.21×10^{-8}
CaCO_3 (aq)	8.86×10^{-5}
CaHCO_3^+	9.28×10^{-5}
Mn^{2+}	1.22×10^{-6}
MnOH^+	4.86×10^{-9}
$\text{Mn}(\text{OH})_2$ (aq)	1.93×10^{-12}
$\text{Mn}(\text{OH})_3^-$	7.70×10^{-17}
$\text{Mn}(\text{OH})_4^{2-}$	3.86×10^{-22}
$\text{Mn}_2\text{OH}^{3+}$	5.93×10^{-15}
$\text{Mn}_2(\text{OH})_3^+$	7.46×10^{-12}
MnCO_3 (aq)	3.23×10^{-6}
MnHCO_3^+	4.89×10^{-7}
H_2CO_3 (aq)	6.36×10^{-5}
HCO_3^-	4.50×10^{-3}
CO_3^{2-}	3.34×10^{-5}
OH^-	1.59×10^{-6}
H^+	6.31×10^{-9}
Species	Initial Concentration [M]
Ca^{2+}	1.60×10^{-3}
Mn^{2+}	1.22×10^{-6}
HCO_3^-	4.50×10^{-3}
H^+	6.31×10^{-9}

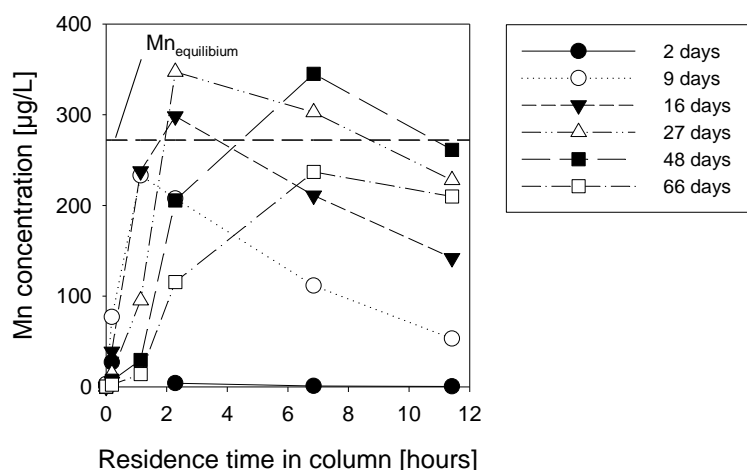


Fig. S2. Profiles of Mn(II) concentration as a function of residence time after 2, 9, 16, 27, 48 and 66 days of the experiment at 20°C and at a flow rate of 0.3 mL/min. Data points refer to SP0, SP1, SP5, SP8, SP11 and SP14. The Mn(II) concentration in equilibrium with rhodochrosite (MnCO_3) is shown with the dashed line (for calculations, see Section 2.4).